



**HAL**  
open science

## Study of nanosecond pulsed DBD applied to electrostatic precipitation: comparison of collection efficiency with AC-DBD

Arthur Claude Aba'a Ndong, Nouredine Zouzou, Eric Moreau

### ► To cite this version:

Arthur Claude Aba'a Ndong, Nouredine Zouzou, Eric Moreau. Study of nanosecond pulsed DBD applied to electrostatic precipitation: comparison of collection efficiency with AC-DBD. International Symposium on Electrohydrodynamics, ISEHD'2014, Jun 2014, Okinawa, Japan. hal-04489454

**HAL Id: hal-04489454**

**<https://hal.science/hal-04489454>**

Submitted on 5 Mar 2024

**HAL** is a multi-disciplinary open access archive for the deposit and dissemination of scientific research documents, whether they are published or not. The documents may come from teaching and research institutions in France or abroad, or from public or private research centers.

L'archive ouverte pluridisciplinaire **HAL**, est destinée au dépôt et à la diffusion de documents scientifiques de niveau recherche, publiés ou non, émanant des établissements d'enseignement et de recherche français ou étrangers, des laboratoires publics ou privés.

# Study of nanosecond pulsed DBD applied to electrostatic precipitation: comparison of collection efficiency with AC-DBD

A. C. Aba'a Ndong, N. Zouzou, E. Moreau  
Institut PPRIME, UPR 3346, CNRS – Université de Poitiers – ISAE-ENSMA  
SP2MI, Téléport 2, Bd. Marie & Pierre Curie, BP 30179  
F86962, Futuroscope Chasseneuil Cedex, FRANCE

**Abstract**— Dielectric barrier discharge based electrostatic precipitators powered by a nanosecond pulsed high voltage is investigated experimentally in this paper. The first goal is to characterize the behavior of the discharge in wire-to-square tube configuration. The second one is to analyze the effect of the voltage pulse polarity on submicrometer particle collection efficiency, before to be compared with AC sine and square voltage waveform HV. The main results show that the positive rise of the voltage pulse favors the formation of a streamer discharge, whereas the negative decay is associated with a corona-glow regime. More, the performance of the ESP is better with the positive pulse voltage due to a filamentary discharge regime, even if the voltage pulse duration is short compared to the waveform period.

**Keywords**— Nanosecond pulsed DBD, AC-DBD, electrostatic precipitation, collection efficiency, granulometry, streamers

## I. INTRODUCTION

Among the means of filtration commonly used in industry, electrostatic precipitators (ESPs) play a significant role to reduce the amount of particles released into the atmosphere [1-3]. For more than a century, researches on corona discharge electrostatic precipitators have made them more efficient and robust. However, there are still too many phenomena deteriorating their performance such as the dependence on particle size, the particle re-entrainment and the back corona discharge, among others [4]. This is why our research group explores a new type of ESPs based on dielectric barrier discharges (DBD) to increase the performance of submicron particles collection.

Recent studies demonstrate the great potential of dielectric barrier discharge based electrostatic precipitators (DBD-ESPs) energized by a low frequency ac high voltage for the collection of submicrometer particles [5-10]. The frequencies range from a few Hz to several kHz, for voltages up to 30 kV. In most cases, the power supply system includes a high voltage linear amplifier with moderate slew rate (less than 1 kV/ $\mu$ s). However, only few studies deal with the use of nanosecond pulsed voltage (rise and fall time in the range of a few ns) for the electrostatic precipitation of particles.

In this paper, the effect of the positive and negative pulsed voltage polarities are examined and compared with AC sine and square voltage waveforms. The analysis relates to the electrical characterization of the discharge and the collection efficiency of submicrometer particles in wire-to-square tube ESP configuration.

## II. EXPERIMENTAL SETUP

The experimental setup is composed of four main modules (Fig. 1): the power supply system and electrical probes, the smoke generator, the particle counting system and the electrostatic precipitator.

Dry clean air is introduced into a custom-designed smoke generator, where the burning of incense sticks generates submicrometer particles. Then, the particles are entrained by the airflow through the ESP. The ESP outlet is connected to a diluter with a controlled additional clean air. Finally, the particle concentration in a diluted sample is measured using an aerosol spectrometer (Palas, Model Wellas-1000). For all experiments, the flow rate inside the ESP is fixed at 2 L/min, resulting in a flow velocity of 0.33 m/s.

The analyzed particles are ranged from 0.18 to 1  $\mu$ m with median particle diameter of 0.28  $\mu$ m. The typical cumulative particle concentration is about  $1.2 \times 10^6$  particles/ $\text{cm}^3$ .

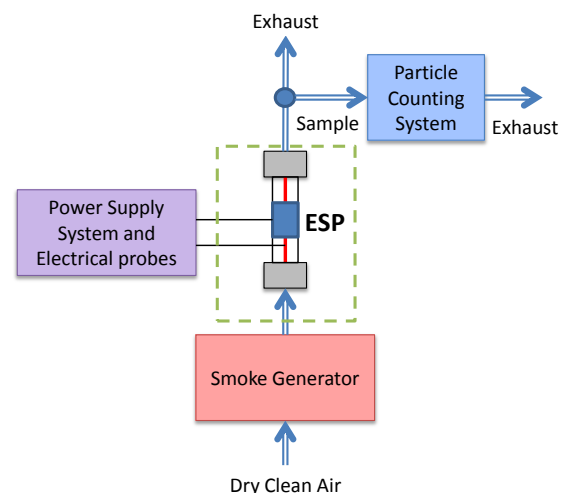


Fig. 1. Schematic illustration of the experimental setup.

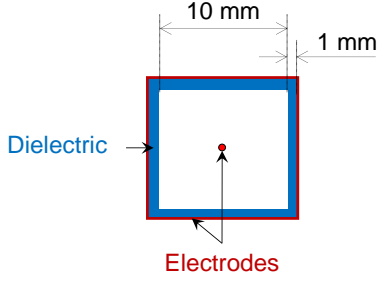


Fig. 2. Cross-view of the DBD-ESP.

The DBD-ESP (Fig. 2) consists of a dielectric square tube (Pyrex, 1 mm thick, 300 mm long, and 10 mm inner ribs) and two electrodes. The active electrode consists of a nickel wire (0.2 mm in diameter) aligned at the central axis of the dielectric tube. The “collecting” electrode (aluminum tape, 20 mm in length and about 70  $\mu\text{m}$  thick) is placed on the external surface of the glass square tube.

The high voltage power supply is composed with an HV solid-state pulser (DEI, model PVX-4110), a DC power supply (Matsuda, model 10P30) and a digital pulse generator (Stanford, model DG645). A single pulser can provide a high voltage pulse up to  $\pm 10$  kV, whose rise and decay times are about 50 ns. By connecting two pulsers (arranged in series opposition), the potential difference between active and collecting electrodes can reach  $\pm 20$  kV. The total current is measured using a fast current transformer (Bergoz, model CT-D1.0) and the potential difference across ESP is measured with twin high voltage probes (LeCroy, model PPE20kV). More details about the experimental setup can be found in [10-11].

### III. RESULTS AND DISCUSSION

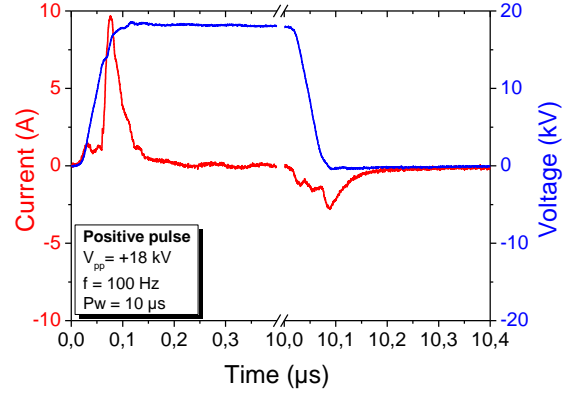
#### A. Electrical behavior

Typical waveforms of the nanosecond pulsed voltage and the associated current are shown in Fig. 3 for both positive and negative polarities. The ESP is supplied with a voltage pulse of  $\pm 18$  kV at a frequency of 100 Hz and a pulse width of 10  $\mu\text{s}$ .

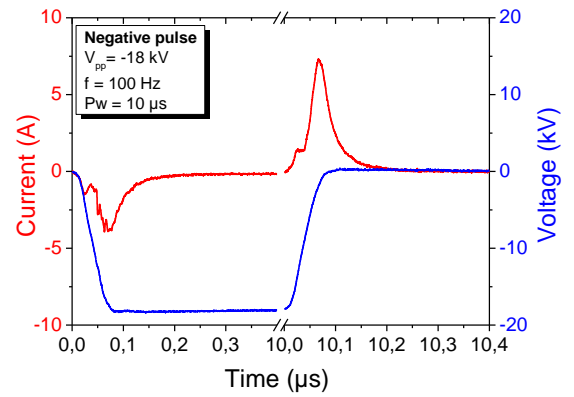
The current waveform shows two peaks well resolved during rise and fall times of the voltage pulse whatever the polarity. No current peak can be observed during the voltage plateau. This is why no data are presented in the range from 0.4 to 10  $\mu\text{s}$ .

The first current peak is due to the deposition of electric charges (with the same polarity than the active electrode) produced by the discharge initiated close to the wire where the electric field is sufficiently intense. During the voltage plateau, the current level decreases rapidly and the discharge is then in its silent period.

When the potential difference between the wire and the charged internal tube surface is one more time sufficient, a new discharge propagates in the gap; this is the second discharge which takes place during the second transition of the voltage. Hence, the second current peak appears.



(a)



(b)

Fig. 3. Typical current waveforms for nanosecond pulsed voltage for (a) positive, and (b) negative polarities.

The shape of the current peaks is nearly similar; however the discharge regimes associated to each one are completely different as we can see in the following section.

Fig. 4 shows the evolution of the power consumption as a function of the applied voltage for both positive and negative pulses. First, the power consumption increases with the voltage. Secondly, the electrostatic precipitator consumes more electric power with the positive polarity.

#### B. Plasma morphology

For simplicity reasons, plasma morphology investigation is carried out in a wire-to-plane geometry, which allows the observation of the discharge in the gap and on the dielectric barrier (Fig. 5). The configuration is composed of two electrodes separated by a dielectric barrier (Pyrex, 1 mm thick, 200 mm in length, and 100 mm in width). The active electrode consists of a nickel wire (0.2 mm in diameter). The collecting electrode (aluminum tape, 20 mm in length and about 70  $\mu\text{m}$  thick) is placed on the lower side of the dielectric barrier and encapsulated. The air gap is fixed at 5 mm in all experiments.

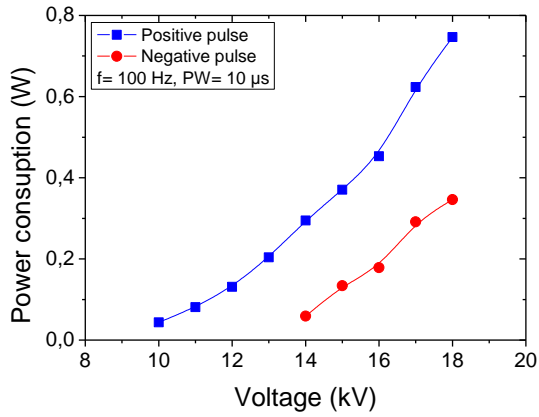


Fig. 4. Power consumption as a function of the applied voltage.

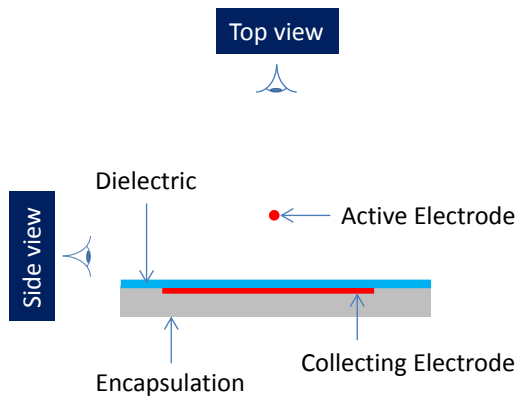


Fig. 5. Cross-view of the wire-to-plane configuration.

The morphology of plasma in wire-to-plane configuration is analyzed using an intensified charge coupled device (ICCD) camera (Princeton Instruments, model Pi-Max2/Gen2) with 1024 x 1024 pixels matrix. Two field views are recorded by placing the ICCD camera in front of the air gap (side view) and then above the dielectric barrier (top view). Even if the camera is able to acquire images with an opening gate width of about 2 ns, we choose to present only images with long opening gate width (about 250 ns) in order to limit the number of images associated to each studied case. Fig. 6 illustrates time windows during which the images are recorded (A, B, C and D).

Fig. 7 shows the plasma morphology during the rise time and fall time of both positive and negative voltage pulses at  $\pm 16$  kV. The plasma form is strongly dependent on the voltage polarity and the slope of the voltage. In the following paragraphs, the effect of every voltage transition is discussed separately.

#### 1) Positive voltage rising (Fig. 7, time window (A))

The side view image shows that the plasma is composed of many filaments distributed along the wire electrode, indicating that the discharge operates in a streamer-like regime. The channels of streamers are straight, well distributed and distinct. Furthermore, the propagation of streamers continues on the dielectric surface until the edge of the lower electrode (top view).

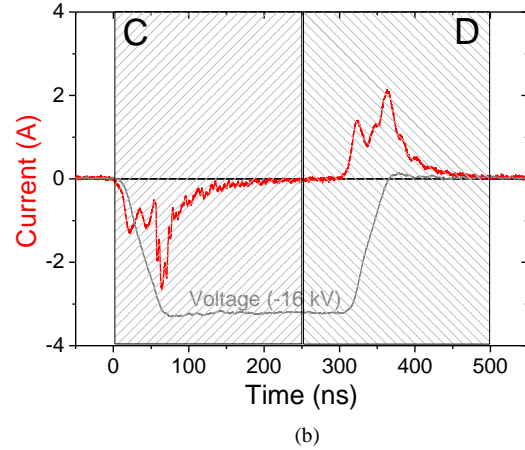
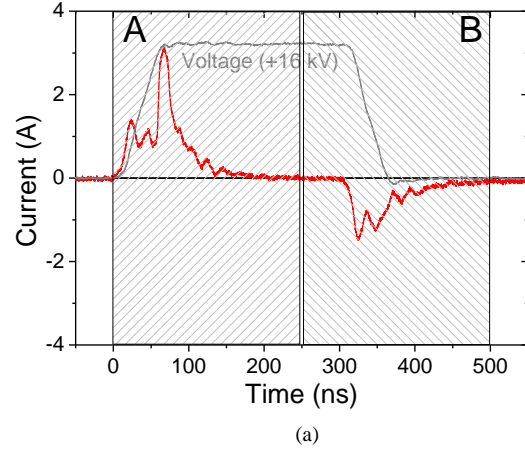


Fig. 6. Temporal location of the opening gate periods of the ICCD camera on the electrical waveforms in the case of (a) positive and (b) negative polarities. Conditions: voltage =  $\pm 16$  kV, frequency = 0.5 Hz, pulse width = 300 ns.

#### 2) Positive voltage falling (Fig. 7(B))

During the falling period of the positive voltage pulse, the plasma is composed of several ionization regions, each one starting from the wire and expanding in the direction of the collecting electrode in a plume shape. However, no significant propagation of the discharge can be observed on the dielectric surface.

#### 3) Negative voltage falling (Fig. 7(C))

The plasma morphology for the negative voltage falling (time window (C)) is quite similar to the one observed during the positive falling voltage (time window (B)). This suggests that the discharge regime is equivalent regardless the polarity of the deposited charge on the dielectric. From the top view image, the plasma is quite diffuse under the wire and did not propagate on the dielectric surface.

#### 4) Negative voltage rising (Fig. 7(D))

The negative voltage rising period is related to the transition from -18 to 0 kV. From the side view image, the plasma morphology is rather similar to the one observed during the positive voltage rising but the filaments are thinner. This is confirmed by the top view image that shows that these filaments do not propagate along the dielectric surface. Also, the top view image shows that the filaments have irregular trajectories.

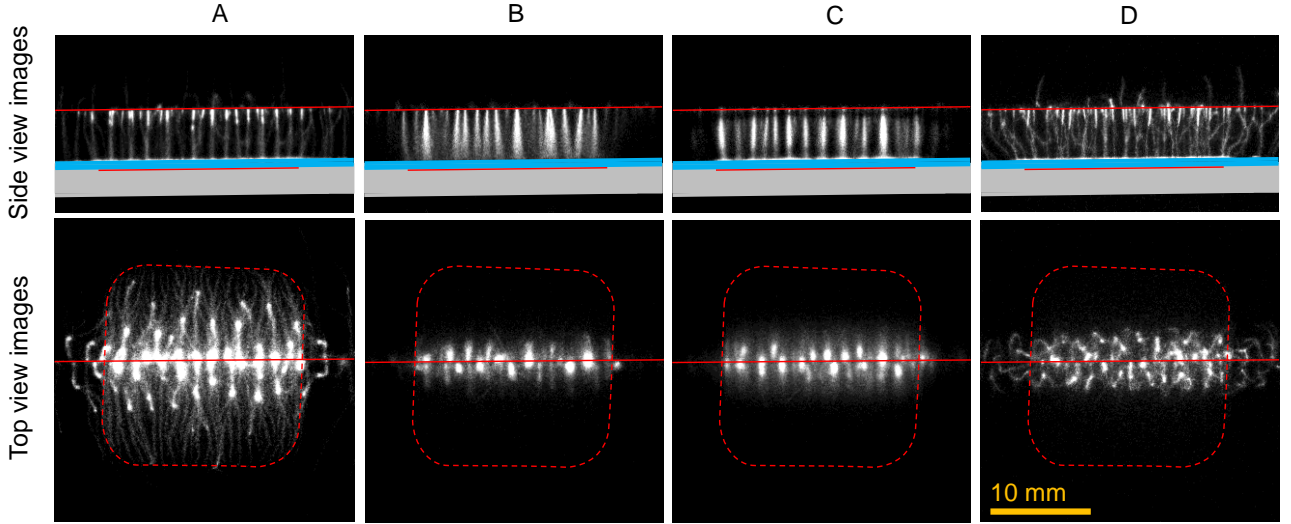


Fig. 7. Top and side views of the plasma morphology corresponding to: (A) positive rising voltage, (B) positive falling voltage, (C) negative falling voltage, and (D) negative rising voltage. Conditions: voltage =  $\pm 16$  kV, frequency = 0.5 Hz, pulse width = 300 ns.

One can conclude that the positive transition of the voltage pulse favors the formation of streamer discharge, whereas the negative transition is associated with a corona-glow discharge.

### C. Collection efficiency

The total number collection efficiency ( $\eta$ ) is defined as follows:

$$\eta = 1 - (N_{\text{ON}} / N_{\text{OFF}}) \quad (1)$$

where  $N_{\text{ON}}$  and  $N_{\text{OFF}}$  are the number of particles per  $\text{cm}^3$  for overall size-classes with and without plasma, respectively, which are measured at the outlet of the wire-to-square tube ESP.

Fig. 8 shows the evolution of the collection efficiency as a function of the average power consumption at a fixed frequency (100 Hz). The effect of the positive and negative pulsed voltage polarities are compared with standard AC sine and square voltage waveforms.

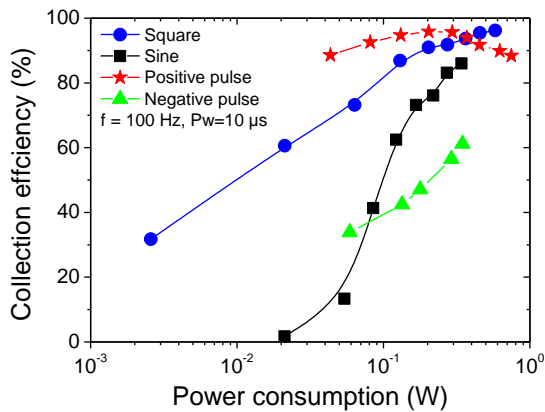


Fig. 8. Evolution of the collection efficiency as a function of the power consumption for different high voltage waveforms.

The performance of the ESP is better at higher power consumption, excepted for the positive pulse at high voltages. In the case of AC voltage, the square wave offers better performance than the sine wave due to strong electric field during both half-cycles.

In the case of negative nanosecond pulsed voltage, the electrostatic precipitation is less effective, because the pulse duration (about 10  $\mu\text{s}$ ) is negligible compared to the signal period (10 ms). Consequently, the drift process of the charged particle is affected by the absence of an external electric field during the most part of the period.

Despite a pulse width which is only 1/1000 of the period and a discharge that develops only over a period of about 1/100 of the pulse (this means that the discharge is activated during only 0.001% of time), the performance of a positive pulse excitation can be better than the square waveform one. This indicates that the particle charging and drift processes operate in a completely different mode compared with the other cases.

## IV. DISCUSSION

With AC voltage, the particles are charged by the ions produced near the wire and driven by the Coulomb forces due to the electric field present in the electrode gap. The same scenario is valid with negative nanosecond pulsed voltage excitation. The discharge, occurring near the wire during the negative transition of the voltage, produces the necessary negative ions for the particle charging process. Then, an extended voltage plateau is required for the electrostatic precipitation of the particle.

In the case of positive pulse, the discharge operates in a filamentary mode during the positive transition of the voltage. Thus, there are two possible scenarios for electrostatic precipitation of submicrometer particles

with filamentary discharges [12]. Particles are charged by the positive ions remaining in the gap after filament propagation, then drift slowly toward the collecting electrode during the voltage plateau. Or else, particles are collected during filament propagation, probably due to the contribution of electrons in the charging process or the effect of the generated pressure wave [12]. Since the pulse width is too short compared to the period, the second scenario seems to be the most plausible. Further experiments with time-resolved particle image velocimetry associated to Schlieren visualizations would allow us to conclude about the physical mechanisms that induce the particle precipitation.

## V. CONCLUSION

In this work, we investigated the collection of submicrometer particles using DBD-ESP powered by nanosecond pulsed high voltage. The first goal was to characterize the behavior of the discharge. The second one was to analyze the effect of the voltage pulse polarity on particle collection, before to be compared with AC sine and square voltage waveforms. The main results of this experimental investigation are as follows.

(1) For both positive and negative voltage pulses, the current waveforms show the existence of two discharges during both rising and falling periods of the voltage.

(2) The positive transition of the voltage pulse favors the formation of streamer discharge, whereas the negative transition is associated with a corona-glow discharge.

(3) The performance of the ESP is better with the positive pulse voltage compared to the negative one and the AC voltage waveforms, which is due to the filamentary discharge regime, even if the voltage pulse duration is short compared to the period (0.001% of time).

Further investigations are necessary to clearly elucidate the mechanisms of interaction between ultrafine particles and streamers during their propagation.

## REFERENCES

- [1] K. R. Parker, *Electrostatic precipitation*, London: Chapman & Hall, 1997.
- [2] A. Mizuno, "Electrostatic precipitation", *IEEE Trans. Dielectr. Electr. Insul.*, vol. 7, pp. 615–624, 2000.
- [3] A. Jaworek, A. Krupa, and T. Czech, "Modern electrostatic devices and methods for exhaust gas cleaning: A brief review", *J. Electrostat.*, vol. 65, pp. 133-155, 2007.
- [4] J. S. Chang, A. J. Kelly and J. M. Crowley, *Handbook of Electrostatic Processes*, New York: Marcel Dekker, 1995.
- [5] B. Dramane, N. Zouzou, E. Moreau, and G. Touchard, "Electrostatic precipitation in wire-to-cylinder configuration: Effect of the high-voltage power supply waveform", *J. Electrostat.*, vol. 67, no. 2-3, pp. 117–122, 2009.
- [6] B. Dramane, N. Zouzou, E. Moreau and G. Touchard, "Electrostatic Precipitation of Submicron Particles using a DBD in axisymmetric and planar configurations", *IEEE Trans. Dielectr. Electr. Insul.*, vol. 16, no. 2, pp. 343–351, 2009.
- [7] N. Zouzou, B. Dramane, E. Moreau, and G. Touchard, "EHD Flow and Collection Efficiency of a DBD-ESP in Wire-to-Plane and Plane-to-Plane Configurations", *IEEE Trans. Ind. Appl.*, vol. 47, no. 1, pp. 336-343, 2011.
- [8] R. Gouri, N. Zouzou, A. Tilmatine, E. Moreau, and L. Dascalescu, "Collection efficiency of submicrometre particles using single and double DBD in a wire-to-square tube ESP", *J. Phys. D: Appl. Phys.*, vol. 44, no. 495201, pp. 1-8, 2011.
- [9] R. Gouri, N. Zouzou, A. Tilmatine and L. Dascalescu, "Enhancement of submicron particle electrostatic precipitation using dielectric barrier discharge in wire-to-square tube configuration", *J. Electrostat.*, vol. 71, no. 3, pp. 240-245, 2013.
- [10] R. Gouri, N. Zouzou, A. Tilmatine, L. Dascalescu, "Study of DBD Precipitator Energized by a Modified Square Waveform Voltage", *IEEE Trans. Dielectr. Electr. Insul.*, vol. 20, no. 5, pp. 1540-1546, 2013.
- [11] A. C. Aba'a Ndong, N. Zouzou, N. Benard, E. Moreau, "Geometrical optimization of a surface DBD powered by a nanosecond pulsed high voltage", *J. Electrostat.*, vol. 71, no. 3, pp. 246-253, 2013.
- [12] N. Zouzou and E. Moreau, "Effect of a filamentary discharge on the particle trajectory in a plane-to-plane DBD precipitator ", *J. Phys. D: Appl. Phys.*, vol. 44, no. 285204, pp. 1-6, 2011.